Comparision between Ga- and N-polarity InGaN solar cells with gradient-In-composition intrinsic layers*

Lin Lu(鲁麟)[1,2,†], Ming-Chao Li(李明潮)[1,2], Chen Lv(吕琛)[2], Wen-Gen Gao(高文根)[1,2], Ming Jiang(江明)[1,2], Fu-Jun Xu(许福军)[3], and Qi-Gong Chen(陈其工)[1,2]

[1] *Anhui Key Laboratory of Detection Technology and Energy Saving Devices, Anhui Polytechnic University, Wuhu* 241000, *China*
[2] *College of Electrical Engineering, Anhui Polytechnic University, Wuhu* 241000, *China*
[3] *Research Center for Wide Gap Semiconductor, School of Physics, Peking University, Beijing* 100871, *China*

(Received 12 April 2016; revised manuscript received 13 June 2016; published online 25 August 2016)

Performances of Ga- and N-polarity solar cells (SCs) adopting gradient-In-composition intrinsic layer (IL) are compared. It is found the gradient ILs can greatly weaken the negative influence from the polarization effects for the Ga-polarity case, and the highest conversion efficiency (η) of 2.18% can be obtained in the structure with a linear increase of In composition in the IL from bottom to top. This is mainly attributed to the adsorptions of more photons caused by the higher In composition in the IL closer to the p-GaN window layer. In contrast, for the N-polarity case, the SC structure with an InGaN IL adopting fixed In composition prevails over the ones adopting the gradient-In-composition IL, where the highest η of 9.28% can be obtained at x of 0.62. N-polarity SC structures are proven to have greater potential preparations in high-efficient InGaN SCs.

Keywords: InGaN, solar cell, polarity

PACS: 88.40.hj, 81.05.Ea, 88.40.jm, 84.60.Jt **DOI:** 10.1088/1674-1056/25/10/108801

1. Introduction

As one of the most important ternary alloys in III-nitrides, $In_xGa_{1-x}N$ (InGaN) has a very high absorption coefficient (10^5 cm^{-1}), high carrier mobility, high radiation resistance and high adjustability for direct band gap ranging from 0.63 eV to 3.4 eV, which makes its absorption cover the wavelength range from 365 nm to 1770 nm (almost the entire solar spectrum), it has become one of the important candidates for preparing photovoltaic devices.[1–5] Although InGaN solar cell (SC) structure has many advantages viewed from a materials point of view, there are many problems and challenges in the actual preparations of device structures. For example, to increase long wavelength absorption efficiency, In composition needs increasing to reduce the band gap of InGaN. However it is hard to control the crystalline quality of InGaN alloy with high In content, where severe phase separation phenomenon will occur and introduce a large number of defects into the InGaN alloy.[6–8] Besides, there is very strong spontaneous and piezoelectric polarization in the InGaN-based SC structure, moreover the polarization will be further enhanced with increasing In composition that can generate a large number of interface charges.[9–11] For the common Ga-polarity SC structure along the [0001] direction, the direction of electric field from the polarization is opposite to that of the built-in electric field, which is much less favorable for carrier collection.[12] Another alternative is to prepare SC structure on an N-polarity template. Chang and Kuo found that the polarization was beneficial for carrier transport in an N-polarity SC structure along the $[000\bar{1}]$ direction.[13] Keller *et al.* also reported that higher In composition InGaN/GaN multiple quantum wells could be obtained using N-polarity structures than Ga-polar ones under the same growth conditions.[14] These imply that polarity can play an important role in structure design for InGaN SC.

The specific structure design adopted for the p–i–n structure is also vital for InGaN high-efficiency SC. Cai *et al.* found there was much better performance in heterojunction SC than homojunction one under the premise of the same depletion region width.[15] However, the detrimental effects of polarization charges and the discontinuity of energy band caused by heterointerfaces will seriously degrade the SC performance. If these effects are not effectively reduced or eliminated, the excellent photovoltaic properties of InGaN SCs will be hard to achieve for practical applications, even if the high-crystalline-quality InGaN SC can be grown. Kuo *et al.* attempted to introduce the step-graded interlayers between the GaN-InGaN interfaces to overcome the above aforementioned critical effects.[16] The other groups also demonstrated that In composition gradient layer as the transitional layer between InGaN and GaN could effectively reduce the barrier height

*Project supported by the National Natural Science Foundation of China (Grant Nos. 61306108, 61172131, and 61271377), the Scientific Research Foundation for the Returned Overseas Chinese Scholars, Ministry of Education of China (Grant No. 2013693), and the Anhui Polytechnic University Funds for Excellent Young Scientists, China (Grant No. 2014YQQ005).

†Corresponding author. E-mail: LLu-wh@qq.com

© 2016 Chinese Physical Society and IOP Publishing Ltd

and lattice mismatch.[17–19] These suggest that when a compositional gradient configuration is employed, the discontinuity of energy band in the heterojunction is reduced, which is beneficial to carriers transporting across the heterojunction, thus enhancing the carrier collection efficiency.

Though many attempts have been made to seek for the optimal structure for InGaN SC, the combination of polarity together with specific structure design, such as compositional gradient configuration in the intrinsic layer (IL), has been less investigated. On one hand, this combination can effectively reduce the discontinuity of the energy band; on the other hand, this combination seems to afford more degree of freedom for tradeoff between carrier generation and transport in the InGaN SC. In this study, the performances of Ga- and N-polarity InGaN SC with gradient In composition IL are simulated and compared with each other.

2. Sample structures and calculation method

Figure 1 shows the schematics of p–i–n SC structures on *c*-plane sapphire substrate for calculation in this study. The thickness of sapphire is set to be 100 μm. A 3-μm-thick n-GaN with electron concentration 5×10^{18}/cm^3 and a 50-nm-thick p-GaN with hole concentration 5×10^{17}/cm^3 are adopted and kept the same for all samples. The major differences among these samples are in IL structure and polarity. Four different IL structures were adopted with Ga- and N-polarity configuration, respectively, as schematically depicted in Fig. 1. Structure A has a p–i–n structure $In_xGa_{1-x}N$ with fixed x as the IL; structure B has an i–InGaN gradient layer with linear variation of In composition from 0 to x in the IL from bottom to top; like structure B, structure C has the IL with linear variation of In composition from x to 0 in the IL; combined with features of structures B and C, In composition first linearly increases from 0 to x and then linearly decreases to 0 for Structure D. All the calculation and simulation are performed through APSYS software, which involves many models, such as drift-diffusion model, nonlocal tunneling model, heterostructure model, multilayer optical model, ray tracing model and so on, to accurately describe the physical processes of semiconductor devices.

For these p–i–n SC structures as shown in Fig. 1, two-dimensional (2D) finite element and Newton iteration techniques are adopted for numerical analysis and simulation based on the heterojunction model and multilayer optical model. Within this scheme, energy band structures, carrier drift-diffusion equation, Poisson's equation and current continuity equation for electrons and holes are self-consistently solved to acquire a variety of properties of InGaN SCs, including the *I*–*V* curves, band structures, distribution of electric potential, etc.

In the simulations, the polarization-induced charges at the interfaces for Ga- and N-polarity cases are strictly calculated by using similar methods developed by Wang *et al.*[20] and Liu *et al.*[21] In addition, AM1.5 incident sunlight is set to be from the top of these structures, and the surface reflectivity is set to be 18%. The Shockley–Read–Hall (SRH) recombination for the InGaN IL that is directly governed by the defect-related nonradiative SRH lifetime is set to be 1 ns,[22,23] and the degree of polarization is set to be 0.9 with considering that the actual polarization charge will be partially screened.

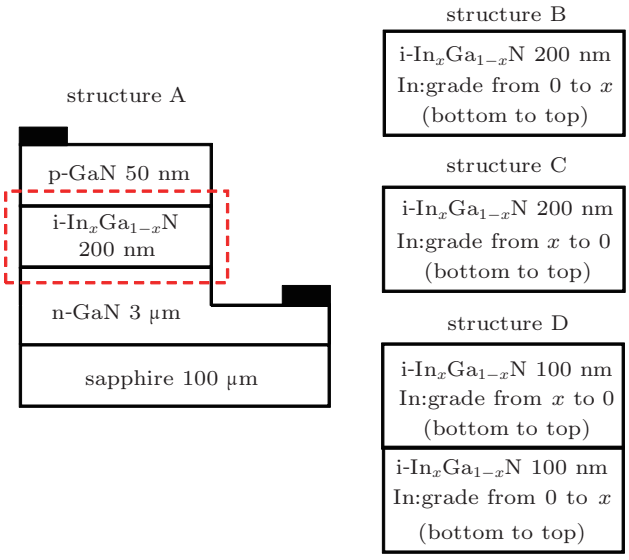


Fig. 1. (color online) Schematics of p–i–n SC structures on *c*-plane sapphire substrate.

3. Results and discussion

Figure 2 shows current density–voltage (*J*–*V*) curves of the Ga- and N-polarity SC's adopting structures A–D with the chosen x value 0.12. The performance parameters are all summarized in Table 1, including the short circuit current density (J_{sc}), open circuit voltage (V_{oc}), filling factor (FF), maximum output power (P_{max}), and conversion efficiency (η). For the Ga-polarity case, compared with structure A, it can be found that structures B–D adopting the gradient ILs have much less J_{sc}, but have much greater V_{oc} and significantly improved η. Among structures B–D, structure B seems to have the best performance, including all the parameters, especially the highest FF value of 91.05% and the η value of 1.95%. In contrast, it can be found that structures A–D have very close V_{oc} values for N-polar SCs, which is different from the case in the Ga-polarity situation. The greatest J_{sc} reaches 1.54 mA/cm^2 for structure A, which is much superior to those for structures B–D. Moreover, there is also the greatest η of 3.08% in structure A, showing superiority to those in structures B–D whose η values are all less than 2%. These indicate that the structure design without adopting the gradient IL seems to be beneficial to high-efficiency SC in N-polarity situation.

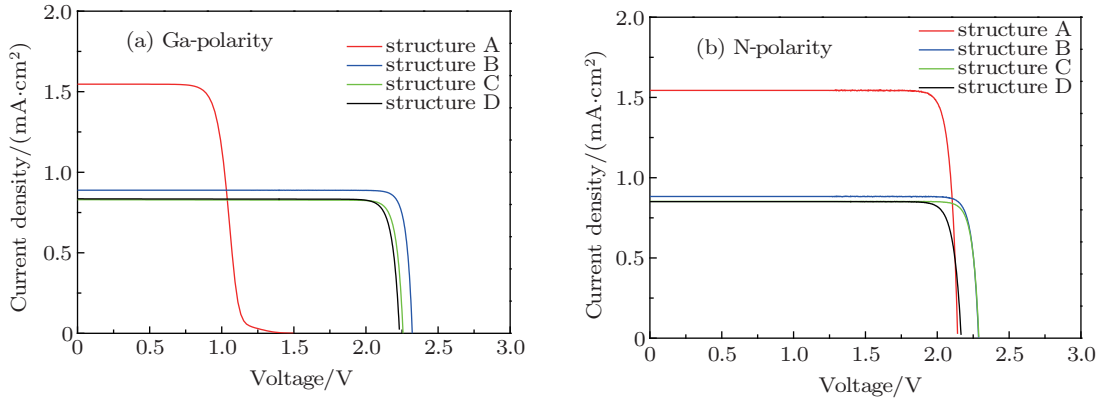


Fig. 2. (color online) J–V curves of (a) Ga-polarity and (b) N-polarity InGaN SC's for the case of $x = 0.12$.

Table 1. Summarized parameters of the Ga- and N-polarity InGaN SCs for the case of i–$In_{0.12}Ga_{0.88}N$ IL. In the table Ga and N denote Ga- and N-polarity, respectively.

Structure	V_{oc}/V		J_{sc}/(mA/cm^2)		FF/%		P_{max}/mW		η/%	
	Ga	N	Ga	N	Ga	N	Ga	N	Ga	N
A	1.49	2.14	1.54	1.54	58.40	89.82	1.34	2.96	1.39	3.08
B	2.32	2.29	0.89	0.88	91.05	90.80	1.88	1.83	1.95	1.90
C	2.26	2.29	0.83	0.85	90.09	90.93	1.69	1.77	1.76	1.84
D	2.23	2.17	0.83	0.85	90.23	88.91	1.67	1.64	1.73	1.71

In order to reveal the influence of the gradient IL on SC, the conduction and valance band structures of structures A–D are calculated for comparison as shown in Fig. 3. For the Ga-polarity case shown in Fig. 3(a), there is much smaller electric field strength (EFS) in structure A in the depletion zone (3.0 μm–3.2 μm) than those in structures B–D, which is reflected by the slope of the conduction or valance band. By calculation, the EFS is 6.88×10^4 V/cm in structure A, much less than the values in structures B–D. The greatest EFS of 1.35×10^5 V/cm occurs in structure B in structures B–D. For Ga-polarity device structures, the polarization electric field is generally opposite to the built-in one for p–i–n InGaN SC. This means that the gradient structure design for the IL is beneficial to weakening the influence from the polarization effect, which also accounts for the greater V_{oc} values in structures with the gradient ILs. In contrast, for the N-polarity case as shown in Fig. 3(b), there are all great slopes of the conduction or valance band for structures A–D and these slopes are very close in magnitude, which means that there is enough net EFS for carrier separation in the depletion layer. The EFS is extracted to be about 1.45×10^5 V/cm in structure A, which is only slightly less than the value of 1.55×10^5 V/cm in structure B. This leads to much greater V_{oc} of structure A in the N-polarity case than that in the Ga-polarity case. Generally, the theoretical maximum V_{oc} is determined by the built-in electric potential difference in p–n junctions, that is to say, with the same depletion region width, the stronger the electric field, the greater the V_{oc} will be. In N-polarity SC design, the polarization electric field commonly has the same direction as the built-in one, which is beneficial to both carrier separation and V_{oc}.

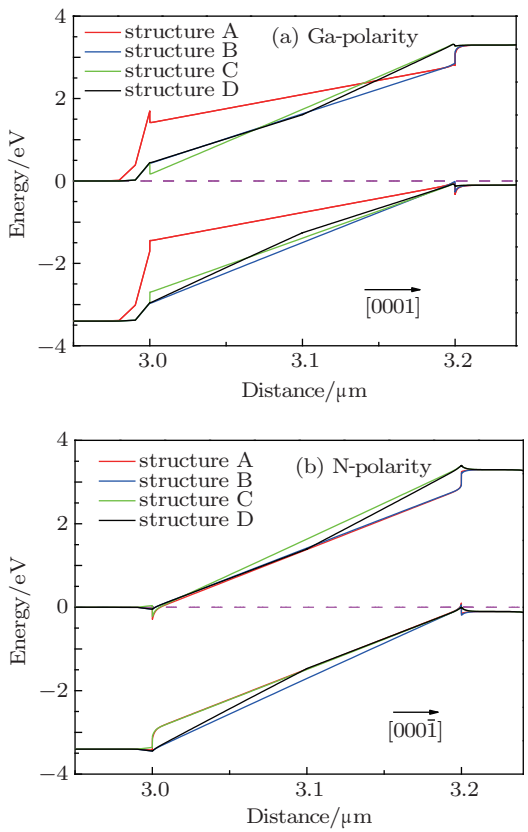


Fig. 3. (color online) Band diagrams at zero bias in the depletion region for (a) Ga-polarity; (b) N-polarity InGaN SC's.

In addition, as shown in Table 1, it can be noted that there are much lower J_{sc} values in structures B–D with the gradient ILs than those in structure A for both Ga- and N-polarity

cases. So, it can be deduced that though the gradient IL design can effectively reduce the barrier height at the interface with GaN layer, which is helpful for carrier transport, this kind of design will inevitablely have the risk of reducing low-energy photon absorption due to the increased absorption band gap originating from the gradient ILs. As is well known, the high-efficiency adsorption of sunlight is vital to high-performance SC, which can be expressed as follows:

$$I(x) = (1-R)I_0 \exp(-\alpha x), \tag{1}$$

where I_0 is the incident light intensity, R is the surface reflectivity, α is the light absorption coefficient, and x is the depth of the incident light. From formula (1), it can be deduced that in the depletion layer, there are more photons in the region closer to the surface which the incident light goes through. For structure B that has a linear variation of In composition from 0 to x in the IL from bottom to top, there is greater In composition in the IL closer to the p-GaN window layer. This corresponds to a gradually narrowing band gap from bottom to top, which is very beneficial to high efficiency adsorption of photons, which is possibly the most important reason why structure B has slightly better performance over structures C and D.

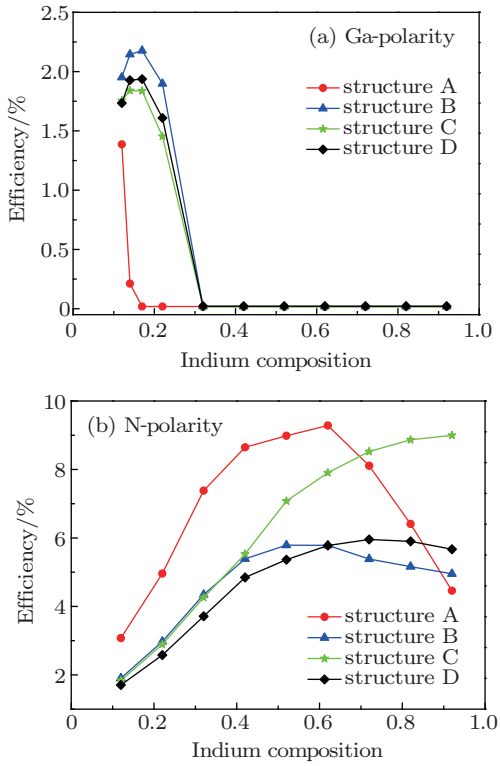


Fig. 4. (color online) Dependences of the conversion efficiency on In composition x of (a) Ga-polarity and (b) N-polarity InGaN SC's.

We further study the performances of these InGaN SC adopting four structures with different values of In composition x, especially dependences of the conversion efficiency η on x as shown in Fig. 4. For the Ga-polarity case, it is found that η drastically decreases with increasing In composition in structure A as shown in Fig. 4(a). In contrast, structures B–D each present first an increase and then a drastic decrease, and they have the top η values severally 2.18%, 1.84%, and 1.94% all at In composition around 0.12. The higher In composition is helpful for the adsorption of sunlight as discussed above, which suggests that when higher In composition (with x much greater than 0.12) is adopted in the IL for Ga-polarity InGaN SC, the stronger polarization effect will be a large obstacle to block collection of the photon-generated carriers, which will have great negative influence on performance of the InGaN SC. Completely unlike the Ga-polarity case as shown in Fig. 4(b), the η values in structures A–D under N-polarity are much larger than those in the Ga-polarity situation. Furthermore, all the η values in structures A, B, and D first increase and then decrease with increasing In composition, exhibiting similar trends. Especially in structure A, it has the top η value 9.28% at x of 0.62, showing much better performance than structures B and D. This suggests that structure A without the gradient IL is more helpful for correcting the photon-generated carriers when adopting N-polarity and also means that N-polarity SC structures have greater potentials in designing and tailoring the physical processes for high-efficient InGaN SC's.

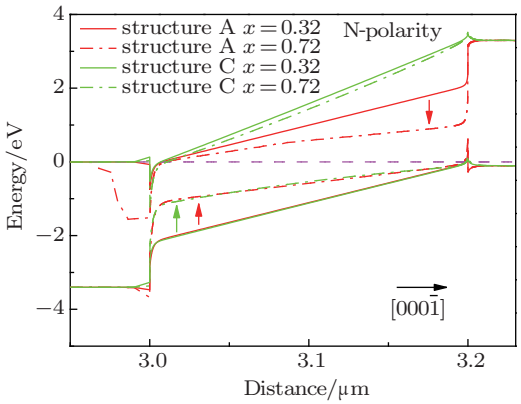


Fig. 5. (color online) Band diagrams at zero bias of the N-polarity InGaN SCs with different contents of In composition.

In addition, it is also worth noting that in structure C, η increases steadily with increasing In composition, and reaches a maximal value of 8.99% at $x = 0.92$ as shown in Fig. 4(b), which apparently differs from those in structures A, B, and D. For better understanding the behaviors of structure C with different x values, we further compare the band structures of N-polarity structures A and C with different x values of 0.32 and 0.72 as shown in Fig. 5. For structure A, the increase of In composition in the IL drives up the valence band near the n-GaN side and pulls down the conduction band near the p-GaN side, which results in a decreased slope of the band of the IL region, implying a weakened EFS. In contrast, in structure C, the valence band near the n-GaN side is lifted up and

the conduction band has little change, corresponding to much less reduced EFS, which means that the EFS weakens more slowly in the depletion layer with increasing In composition x, resulting in much less reduction in the V_{oc}. So, when adopting structure C for InGaN SC design, the positive effect of increasing the short circuit current density caused by the increase of In composition in the IL prevails over the negative one coming from reducing the open circuit voltage. Therefore, it can be recognized that the increase of In composition in the IL can effectively increase the photon absorption and the short circuit current density J_{sc} as well, whereas this will also reduce the open circuit voltage V_{oc}, and a reasonable structure adopted for the tradeoff between these two aspects is vital to improving the performances of InGaN SC's.

4. Conclusions

In this study, the performances of Ga- and N-polarity SCs adopting gradient-In-composition IL are compared. It is found that the gradient ILs can greatly weaken the negative influence from the polarization for the Ga- polarity case, and the highest η of 2.18% can be obtained in the structure with a linear increase of In composition in the IL from bottom to top. This is mainly attributed to the adsorptions of more photons caused by the higher In composition closer to the p-GaN window layer. In contrast, for the N-polarity case, the SC structure with InGaN IL adopting a fixed quantity of In composition prevails over the ones adopting the gradient-In-composition IL, where the highest η of 9.28% can be obtained at $x = 0.62$. The N-polarity SC structures are proven to have greater potential applications in preparing high-efficient InGaN SCs.

References

[1] Hamzaoui H, Bouazzi A S and Rezig B 2005 *Sol. Energ. Mater. Sol. Cells* **87** 595
[2] Zhou M and Zhao D G 2012 *Acta Phys. Sin.* **61** 168402 (in Chinese)
[3] Wu J, Walukiewicz W, Yu K M, Shan W and Ager J W 2003 *J. Appl. Phys.* **94** 6477
[4] Xing Y H, Han J, Liu J P, Deng J, Niu N H and Shen G D 2007 *Acta Phys. Sin.* **56** 7295 (in Chinese)
[5] Zhao B J, Chen X, Ren Z W, Tong J H, Wang X F, Li D W, Zhuo X J, Zhang J, Yi H X and Li S T 2013 *Chin. Phys. B* **22** 088401
[6] Elmasry N A, Piner E L, Liu S X and Bedair S M 1998 *Appl. Phys. Lett.* **72** 40
[7] McCluskey M D, Romano L T, Krusor B S, Bour D P, Johnson N M and Brennan S 1998 *Appl. Phys. Lett.* **72** 1730
[8] Doppalapudi D, Basu S N, Ludwig K F and Moustakas T D 1998 *J. Appl. Phys.* **84** 1389
[9] Fiorentini V, Bernardini F and Ambacher O 2002 *Appl. Phys. Lett.* **80** 1204
[10] Yang J, Zhao D G, Jiang D S, Liu Z S, Chen P, Li L, Wu L L, Le L C, Li X J, He X G, Wang H, Zhu J J, Zhang S M, Zhang B S and Yang H 2013 *Chin. Phys. B* **22** 098801
[11] Yu L, Zhang Y W, Li K, Pi H, Diao J S, Wang X F, Hu W X, Zhang C Z, Song W D, Shen Y and Li S T 2015 *Chin. Phys. B* **24** 077801
[12] Li Z Q, Lestradet M, Xiao Y G and Li S 2011 *Phys. Status Solidi* **208** 928
[13] Chang J Y and Kuo Y K 2012 *J. Appl. Phys.* **112** 033109
[14] Keller S, Fichtenbaum N A, Furukawa M, Speck J S, Denbaars S P and Mishra U K 2007 *Appl. Phys. Lett.* **90** 191908
[15] Cai X M, Wang Y, Chen B H, Liang M M, Liu W J, Zhang J Y, Lv X Q, Ying L Y and Zhang B P 2013 *IEEE Photon. Technol. Lett.* **25** 59
[16] Kuo Y K, Chang J Y and Shih Y H 2012 *IEEE J. Quantum Electron.* **48** 367
[17] Jeng M J 2012 *Int. J. Photoenergy* **8** 7073
[18] Nacer S and Aissat A 2015 *Optik* **126** 3594
[19] Brown G F, Iii J W A, Walukiewicz W and Wua J 2010 *Sol. Energ. Mater. Sol. Cells* **94** 478
[20] Wang L, Hu W D, Chen X S and Lu W 2012 *J. Electron. Mater.* **41** 2130
[21] Liu C, Wang C, Chen XY and Yang Y 2015 *Opt. Quantum Electron.* **47** 2479
[22] Zhu D, Xu J R, Noemaun A N, Kim J K, Schubert E F, Crawford M H and Koleske D D 2009 *Appl. Phys. Lett.* **94** 081113
[23] Chen J R, Lu T C, Kuo H C, Fang K L, Huang K F, Kuo C W, Chang C J, Kuo C T and Wang S C 2010 *IEEE Photon. Technol. Lett.* **22** 860